Available online at www.sciencedirect.com
SCIENCE DIRECT®
Journal of Organometallic Chemistry 691 (2006) 1560–1572
Journal of Organometallic Chemistry
www.elsevier.com/locate/jorganchem

A ferrocenyl-bridged intramolecularly coordinated bis(diorganostannylene): Synthesis, molecular structure and reactivity of [4-*t*-Bu-2,6-{P(O)(O-*i*-Pr)$_2$C$_6$H$_2$Sn}C$_5$H$_4$]$_2$Fe ☆

Markus Henn [a], Markus Schürmann [a], Bernard Mahieu [b], Piero Zanello [c], Arnaldo Cinquantini [c], Klaus Jurkschat [a,*]

[a] *Lehrstuhl für Anorganische Chemie II der Universität Dortmund, D-44221 Dortmund, Germany*
[b] *Laboratoire de Chimie Structurale (CSTR), Université de Louvain, B-1348 Louvain-la-Neuve, Belgium*
[c] *Department of Chemistry, University of Siena, Via Aldo Moro, I-53100 Siena, Italy*

Received 7 December 2005; accepted 8 December 2005
Available online 19 January 2006

Dedicated to Professor Herbert Schumann.

Abstract

The intramolecularly coordinated heteroleptic stannylene [4-*t*-Bu-2,6-{P(O)(O-*i*-Pr)$_2$}$_2$C$_6$H$_2$]SnCl serves as synthon for the synthesis of the ferrocenyl-bridged bis(diorganostannylene) [4-*t*-Bu-2,6-{P(O)(O-*i*-Pr)$_2$}$_2$C$_6$H$_2$SnC$_5$H$_4$]$_2$Fe (**1**) which in turn reacts with W(CO)$_6$ and Cr(CO)$_4$(C$_7$H$_8$) to provide the corresponding transition metal complexes [4-*t*-Bu-2,6-{P(O)(O-*i*-Pr)$_2$}$_2$C$_6$H$_2$Sn{W(CO)$_5$}C$_5$H$_4$]$_2$Fe (**2**) and [4-*t*-Bu-2,6-{P(O)(O-*i*-Pr)$_2$}$_2$C$_6$H$_2$SnC$_5$H$_4$]$_2$Fe · Cr(CO)$_4$ (**3**), respectively. Reaction of compound **1** with sulphur and atmospheric moisture gave, under partial tin–carbon and oxygen–carbon bond cleavage, a tetranuclear organotin-oxothio cluster **5**. All compounds were characterized by ^{1}H, ^{13}C, ^{31}P, and ^{119}Sn NMR, and IR spectroscopy, as well as by single-crystal X-ray diffraction analysis. Compounds **1** and **3** were also investigated by Mössbauer spectroscopy. Cyclovoltametric studies reveal the influence of the organostannyl moieties on the redox-behaviour of compounds **1**–**3** in comparison with unsubstituted ferrocene.

Keywords: Stannylene; Ferrocene; Chromium; Tungsten; Mössbauer spectroscopy; Cyclovoltametry

1. Introduction

The first stable organostannylene, namely bis(cyclopentadienyl)tin(II), SnCp$_2$, was synthesized by Fischer and Grubert [1,2]. It is monomeric in solution and in the solid state and shows a bent sandwich-type structure. The first diorganostannylene exclusively containing Sn–C σ-bonds, namely Sn[CH(SiMe$_3$)$_2$]$_2$, was reported by Lappert and co-workers [3]. This compound is remarkable as it is a dimer in the solid state but undergoes homolytic tin–tin bond dissociation in solution. Both works initiated enormous and still ongoing research activities not only in organotin(II) chemistry but also in the chemistry of their silicon, germanium, and lead congeners, and beyond [5–19]. In course of these studies chemists learned that stabilization of stannylenes can be achieved either kinetically by bulky substituents [4,20–24] and/or thermodynamically by intramolecular coordination of donor atoms such as nitrogen, phosphorus, and oxygen [25–36]. Both methods also made possible the isolation of heteroleptic stannylenes of type RSnX (R = organic substituent, X = halogen, diorganoamide, H, etc.) [37–43] which in turn served as

☆ This work contains part of the PhD thesis of Markus Henn, Dortmund University, 2004. Parts of this work were first presented at 11th International Conference on the Coordination and Organometallic Chemistry of Germanium, Tin, and Lead, ICCOC-GTL-11, 27 June–2 July, 2004, Santa Fe, NM, USA, Book of Abstracts O54.

* Corresponding author. Tel.: +49 231 7553800; fax: +49 231 7555048.
E-mail address: klaus.jurkschat@uni-dortmund.de (K. Jurkschat).

0022-328X/$ - see front matter © 2005 Elsevier B.V. All rights reserved.
doi:10.1016/j.jorganchem.2005.12.026

synthons for subsequent reactions. Notably, in contrast to the great number of well-characterized mononuclear organotin(II) compounds, to the best of our knowledge, compounds (**A**) [44] and (**B**) [45,46] are the only spacer-bridged di-, respectively, trinuclear stannylenes reported so far (Chart 1). In principle, spacer-bridged bis(organostannylenes) might hold potential as chelate ligands in transition metal chemistry, provided that the spacer is well-designed.

Ferrocene-substituted organotin(IV) compounds such as ferrocenophanes (compound **C** in Chart 1) [47–50] are known for some time. They are of interest for the synthesis of redox-active inorganic polymers such as compound **D**. In this context, it is surprising that only one representative of a ferrocene-containing organostannylene is known so far (compound **E** in Chart 1) [35].

In course of a systematic study on phosphorus-containing O,C,O-coordinating pincer-type ligands and their application to the synthesis of both main group and transition metal derivatives we have prepared the intramolecularly coordinated heteroleptic stannylenes of type (**F**) (Chart 1) [41]. Especially the *i*-propoxy-substituted representative of **F** is available in good yields, crystallizes easily and, as result of its high stability, can be handled without problems. It proved to be an ideal heteroleptic stannylene to study subsequent reactions at the Sn–Cl function. Here, we report its reaction with 1,1′-dilithioferrocene to give the first ferrocenyl-bridged bis(organostannylene) and subsequent reactions of the latter with transition metal carbonyls. Moreover, in course of the attempt to perform an oxidative addition reaction with sulphur of the bis(diorganostannylene) we noticed formation of an unprecedented tetranuclear organotin(IV) compound showing a sulphur-containing ladder-type structure.

2. Experimental

General. All solvents including tetramethyl ethylene diamine (hereafter referred to as TMEDA) were dried by standard procedures and freshly distilled prior to use. All reactions were carried out under argon atmosphere using Schlenk techniques.

IR spectra (cm^{-1}) were recorded on a Bruker IFS 28 spectrometer. Bruker DPX-300 and DRX-400 spectrometers were used to obtain ^{1}H (400.13 MHz), ^{13}C (100.63 MHz), ^{31}P (121.49 MHz, 161.98 MHz), and ^{119}Sn (111.92 MHz, 149.18 MHz) NMR spectra. ^{1}H, ^{13}C, ^{31}P, and ^{119}Sn NMR chemical shifts δ are given in ppm and were referenced to Me_4Si (^{1}H, ^{13}C), Me_4Sn (^{119}Sn), and H_3PO_4 (85%, ^{31}P), respectively. NMR spectra were recorded at room temperature. Elemental analyses were performed on a LECO-CHNS-932 analyser. The Möss-

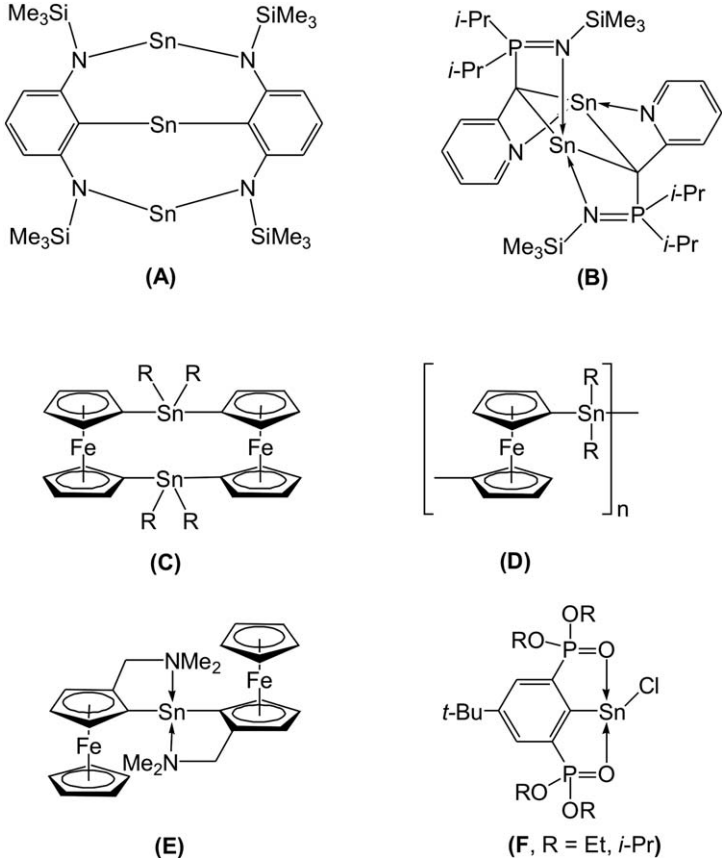

Chart 1.

bauer spectra were recorded in constant acceleration mode on a home-made instrument, designed and built by the Instituut voor Kern-& Stralingsfysica (IKS), Leuven. The isomer shifts refer to a source of $Ca^{119m}SnO_3$ from Amersham, UK, samples being maintained at 90 ± 2 K. The data were treated with a least-squares iterative program de-convoluting the spectrum into a sum of Lorentzians. Materials and apparatus for electrochemical and spectro-electrochemical studies have been described elsewhere [51]. Potential values are referred to the saturated calomel electrode (SCE). Under the experimental conditions employed, the one-electron oxidation of ferrocene occurs at $E^{0'} = +0.51$ V.

The organostannylene [4-*t*-Bu-2,6-{P(O)(O*i*-Pr)$_2$}$_2$-C$_6$H$_2$]SnCl was synthesized as described [52]. Details including its molecular structure will be reported in a forthcoming paper.

2.1. Crystallography

Intensity data for the crystals were collected on a Nonius KappaCCD diffractometer with graphite-monochromated MoKα (0.71073 Å) radiation at 173(1) K. The data collection covered almost the whole sphere of reciprocal space with 3 (**1**, **2**, **5**) and 4 (**3**) sets at different *k*-angles with 159 (**1**), 383 (**2**), 381 (**3**), and 266 (**5**) frames via ω-rotation ($\Delta/\omega = 1°$) (**2**, **3**, **5**) and ($\Delta/\omega = 2°$) (**1**) at two times 20s (**1**), 25s (**3**), 30s (**5**), and 75s (**2**) per frame. The crystal-to-detector distances were 3.4 cm. Crystal decays were monitored by repeating the initial frames at the end of data collection. The data were not corrected for absorption effects. Analyzing the duplicate reflections there were no indications for any decay. The structure was solved by direct methods SHELXS97 [53] and successive difference Fourier syntheses. Refinement applied full-matrix least-squares methods SHELXL97 [54].

The H atoms were placed in geometrically calculated positions using a riding model with isotropic temperature factors constrained at 1.2 for non-methyl and at 1.5 for methyl groups times U_{eq} of the carrier C atom.

The *i*-propoxy groups are disordered in **1** (s.o.f. 0.4 (C(46′)), 0.5 (C(9), C(9′), C(43), C(43′)), 0.6 (C(46))), in **3** (s.o.f. 0.4 C(33′)), 0.5 (O(3′), O(3″), C(47), C(53), C(54), O(3′B), O(3″B), C(47′), C(53′), C(54′) 0.6 C(33′)), in **5** (s.o.f. 0.4 C(38′), C(39′), 0.6 C(38), C(39)). *t*-Bu groups are disordered in **1** (s.o.f. 0.2 C(8′), C(10′), 0.5 C(9), C(9′), 0.8 C(8), C(10)), in **2** (s.o.f. 0.4 C(8′), C(9′), C(10′), 0.6 C(8), C(9), C(10)), in **3** (s.o.f. 0.4 C(18′), C(19′), C(20′), 0.6 C(18), C(19), C(20)). A W(CO)$_5$ group is disordered in **2** (s.o.f. 0.45 O(16), C(16), O(19), C(19), 0.55. O(16′), C(16′), O(19′), C(19′)).

All solvent molecules toluene were refined with a set of restraints to aid in modeling the disorder (AFIX 66 for aromatic rings and DFIX 1.540(1) for methyl aryl distances), whereas only in **1** (C(51) > C(57)) and **3** they were anisotropically refined. Occupancies of 0.2 (C(51′) > C(57′)) and 0.8 (C(51) > C(57)) in **1**, of 1 (C(41) > C(47)) in **2**, of 0.5 (C(81) > C(87)) and 1 (C(61) > C(67), C(71) > C(77)) in **3**, of 0.2 (C(61) > C(67)), 0.25 (C(51) > C(57), C(51′) > C(57′)), 0.8 (C(41) > C(47)) in **5** were applied for refinement of the solvent molecules toluene.

Atomic scattering factors for neutral atoms and real and imaginary dispersion terms were taken from International Tables for X-ray Crystallography [55]. The figures were created by SHELXTL [56]. Crystallographic data are given in Table 1, selected bond distances and angles in Tables 2 (**1**, **2**), 3 (**3**), and 4 (**5**).

2.1.1. Synthesis of [4-t-Bu-2,6-{P(O)(O-i-Pr)$_2$}$_2$C$_6$H$_2$SnC$_5$H$_4$]$_2$Fe (1)

At −78 °C, to a magnetically stirred solution of [4-*t*-Bu-2,6-{P(O)(O-*i*-Pr)$_2$}$_2$C$_6$H$_2$]SnCl (2.90 g, 4.7 mmol) in THF (70 ml) was added in small portions 1,1′-dilithioferrocene · TMEDA (0.71 g, 2.3 mmol) over a period of 60 min. The reaction mixture was stirred for 12 h during which it warmed to room temperature. After the THF had been removed in vacuo, toluene (100 ml) was added to the residue and the reaction mixture was stirred for 10 min followed by filtration from insoluble inorganic salts. The filtrate was reduced in vacuo to a volume of approximately 20 ml and kept overnight at −30 °C to give 2.54 g (82%) of compound **1** as orange crystals which decompose at 170 °C.

^{1}H NMR (400.13 MHz, C$_6$D$_6$): δ 0.99 (d, 12H, CH(C*H*$_3$)$_2$, $J(^1H–^1H) = 6.3$ Hz), 1.03 (d, 12H, CH(C*H*$_3$)$_2$, $J(^1H–^1H) = 6.3$ Hz), 1.17 (s, 18H, C(C*H*$_3$)$_3$), 1.23 (d, 12H, CH(C*H*$_3$)$_2$, $J(^1H–^1H) = 6.3$ Hz), 1.34 (d, 12H, CH(C*H*$_3$)$_2$, $J(^1H–^1H) = 6.3$ Hz), 4.62–4.79 (complex pattern, 12H, C*H*(CH$_3$)$_2$ + C$_5$*H*$_4$), 5.00 (s, 4H, C$_5$*H*$_4$), 8.02 (d, 4H, *CH*$_{aryl}$, $^3J(^{31}P–^1H) = 13.3$ Hz). ^{13}C{^{1}H} NMR (100.63 MHz, C$_6$D$_6$): δ 23.6 (complex pattern, CH(*C*H$_3$)$_2$), 23.9 (complex pattern, CH(*C*H$_3$)$_2$), 24.3 (complex pattern, CH(*C*H$_3$)$_2$), 31.0 (s, C(*C*H$_3$)$_3$), 34.4 (s, *C*(CH$_3$)$_3$), 70.7 (s, *C*$_5$*H*$_{4meta}$), 71.1 (d, *C*H(CH$_3$)$_2$), 71.3 (d, *C*H(CH$_3$)$_2$), 74.5 (s, *C*$_5$*H*$_{4ortho}$), 96.0 (s, *C*$_5$*H*$_{4ipso}$), 131.2 (dd, *C*$_{3/5aryl}$, $^2J(^{13}C–^{31}P) = 17.0$ Hz, $^4J(^{13}C–^{31}P) = 4.4$ Hz), 133.2 (dd, *C*$_{2/6aryl}$, $^1J(^{13}C–^{31}P) = 192.9$ Hz, $^3J(^{13}C–^{31}P) = 24.3$ Hz), 149.0 (t, *C*$_{4aryl}$, $^3J(^{13}C–^{31}P) = 12.9$ Hz), 187.4 (t, *C*$_{1aryl}$, $^2J(^{13}C–^{31}P) = 37.9$ Hz). ^{31}P{^{1}H} NMR (161.98 MHz, C$_6$D$_6$): δ 33.9 ($J(^{31}P–^{119/117}Sn) = 90.8$ Hz). ^{119}Sn{^{1}H} NMR (111.92 MHz, D$_2$O-Kap.): δ 117 ($J(^{31}P–^{119}Sn) = 92$ Hz). IR (KBr): $\tilde{\nu} = 1199$ cm^{-1} (P═O), 1179 cm^{-1} (P═O). Mössbauer spectroscopy: I.S. = 2.61 mm/s, Q.S. = 4.01 mm/s. Elemental analyses calculated for C$_{54}$H$_{86}$P$_4$O$_{12}$Sn$_2$Fe (1344.41 g/mol): C, 48.24; H, 6.45. Found: C, 47.6; H, 6.6%.

2.1.2. Synthesis of [4-t-Bu-2,6-{P(O)(O-i-Pr)$_2$}$_2$C$_6$H$_2$Sn{W(CO)$_5$}C$_5$H$_4$]$_2$Fe (2)

A solution of tungsten hexacarbonyl, W(CO)$_6$, (1.00 g, 2.8 mmol) in THF (242 ml) was irradiated for 2 h with UV-light (Hg-lamp, 150 W) and the carbon monoxide formed during this time was collected and its volume measured to amount 65 ml. Part of this solution (71 ml)

Table 1
Crystallographic data for **1**–**3** and **5**

	1	**2**	**3**	**5**
Formula	$C_{54}H_{86}FeO_{12}P_4Sn_2 \cdot 2C_7H_8$	$C_{64}H_{86}FeO_{22}P_4Sn_2W_2 \cdot 2C_7H_8$	$C_{58}H_{86}CrFeO_{12}P_4Sn_2 \cdot 2.5C_7H_8$	$C_{58}H_{80}Fe_2O_{14}P_4S_2Sn_4 \cdot 3C_7H_8$
Formula weight	1528.61	2176.41	1738.71	2052.08
Crystal system	Triclinic	Monoclinic	Triclinic	Triclinic
Crystal size (mm)	$0.15 \times 0.15 \times 0.15$	$0.10 \times 0.08 \times 0.08$	$0.13 \times 0.13 \times 0.10$	$0.12 \times 0.10 \times 0.10$
Space group	$P\bar{1}$	$C2/c$	$P\bar{1}$	$P\bar{1}$
a (Å)	11.2756(2)	33.8542(5)	13.7012(5)	12.1921(6)
b (Å)	13.0592(3)	13.0525(2)	15.3976(6)	13.6002(7)
c (Å)	14.6735(5)	20.6756(3)	20.2986(9)	14.9386(9)
α (°)	101.8874(9)	90	74.353(3)	89.6881(14)
β (°)	110.0257(10)	101.0201(7)	84.587(2)	72.9584(15)
γ (°)	105.4518(11)	90	87.933(2)	72.619(3)
V (Å^3)	1848.27(7)	8967.4(2)	4105.0(3)	2251.0(2)
Z	1	4	2	1
ρ_{calcd} (Mg/m^3)	1.373	1.612	1.407	1.514
μ (mm^{-1})	1.006	3.400	1.042	1.579
$F(000)$	792	4320	1794	1034
θ Range (°)	2.93–27.49	3.28–27.47	2.99–27.47	3.12–25.37
Index ranges	$-14 \leqslant h \leqslant 14$; $-16 \leqslant k \leqslant 16$; $-19 \leqslant l \leqslant 19$	$-43 \leqslant h \leqslant 43$; $-16 \leqslant k \leqslant 16$; $-26 \leqslant l \leqslant 26$	$-17 \leqslant h \leqslant 17$; $-19 \leqslant k \leqslant 19$; $-26 \leqslant l \leqslant 26$	$-14 \leqslant h \leqslant 14$; $-15 \leqslant k \leqslant 15$; $-17 \leqslant l \leqslant 17$
Number of reflections collected	18,585	33,190	47,706	17,645
Completeness to θ_{max}	99.3	97.9	98.2	97.3
Number of independent reflections/R_{int}	8427/0.022	10,064/0.031	18,475/0.051	8064/0.054
Number of reflections observed with ($I > 2\sigma(I)$)	6132	5407	8400	4587
Number of refined Parameters	455	509	973	461
Goodness-of-fit (F^2)	0.987	0.901	0.829	1.023
R_1 (F) ($I > 2\sigma(I)$)	0.0298	0.0478	0.0438	0.0618
wR_2 (F^2) (all data)	0.0676	0.1168	0.0926	0.1773
$(\Delta/\sigma)_{max}$	0.001	0.001	0.001	0.001
Largest difference in peak/hole (e/Å^3)	0.612/−0.435	2.185/−3.120	0.763/−0.598	0.949/−0.656

containing $W(CO)_5 \cdot THF$ was added drop-wise to a magnetically stirred solution of [4-*t*-Bu-2,6-{P(O)-(O-*i*-Pr)$_2$}$_2$C$_6$H$_2$SnC$_5$H$_4$]$_2$Fe (0.562 g, 0.42 mmol) in THF (40 ml). After the reaction mixture had been stirred for 12 h at room temperature part of the THF (80 ml) was removed in vacuo to cause precipitation of compound **2** (0.468 g, 56%) as orange crystals which decompose at 165 °C. Single crystals of compound **2** were obtained as its toluene solvate $\mathbf{2} \cdot C_7H_8$ from a toluene solution.

^{1}H NMR (400.13 MHz, THF-d^8): δ 1.03 (d, 12H, CH(CH_3)$_2$, J(^{1}H–^{1}H) = 6.0 Hz), 1.19 (d, 12H, CH(CH_3)$_2$, J(^{1}H–^{1}H) = 6.0 Hz), 1.22 (d, 12H, CH(CH_3)$_2$, J(^{1}H–^{1}H) = 6.0 Hz), 1.37 (s + d, 30H C(CH_3)$_3$ + CH(CH_3)$_2$), 4.01 (s, 4H, C$_5H_4$), 4.32–4.37 (complex pattern, 4H, CH(CH$_3$)$_2$), 4.60 (s, 4H, C$_5H_4$), 4.75–4.80 (complex pattern, 4H, CH(CH$_3$)$_2$), 7.95 (d, 4H, *CH*$_{aryl}$, ^3J(^{31}P–^{1}H) = 12.8 Hz). ^{13}C{^{1}H} NMR (100.63 MHz, THF-d^8): δ 22.7–22.9 (complex pattern, CH(*C*H$_3$)$_2$), 23.1 (complex pattern, CH(*C*H$_3$)$_2$), 30.2 (s, C(*C*H$_3$)$_3$), 34.5 (s, *C*(CH$_3$)$_3$), 70.8 (s, *C$_5H_{4meta}$*), 72.3–72.5 (complex pattern, *C*H(CH$_3$)$_2$), 73.8 (s, *C$_5H_{4ortho}$*, ^2J(^{13}C–$^{119/117}$Sn) = 50.1 Hz), 87.8 (s, *C$_5H_{4ipso}$*), 131.4 (dd, *C$_{3/5aryl}$*, ^2J(^{13}C–^{31}P) = 15.1 Hz, ^4J(^{13}C–^{31}P) = 4.4 Hz), 132.2 (dd, *C$_{2/6aryl}$*, ^1J(^{13}C–^{31}P) = 189.0 Hz, ^3J(^{13}C–^{31}P) = 20.9 Hz), 152.0 (t, *C$_{4aryl}$*, ^3J(^{13}C–^{31}P) = 12.6 Hz), 169.7 (t, *C$_{1aryl}$*, ^2J(^{13}C–^{31}P) = 27.2 Hz), 200.3 (s, *C*O, ^2J(^{13}C–$^{119/117}$Sn) = 60.7 Hz, ^1J(^{13}C–^{183}W) = 122.9 Hz), 202.5 (s, *C*O). ^{31}P{^{1}H} NMR (161.98 MHz, THF-d^8): δ 9.3 (J(^{31}P–$^{119/117}$Sn) = 106 Hz). ^{119}Sn{^{1}H} NMR (149.21 MHz, THF-d^8): δ 88 (J-(^{31}P–^{119}Sn) = 108 Hz, J(^{119}Sn–W) = 1099 Hz). IR (KBr): $\tilde{\nu}$ = 1183 cm^{-1} (P=O), 1900 cm^{-1} (CO), 1931 cm^{-1} (CO), 2051 cm^{-1} (CO). Elemental analyses calculated for $C_{64}H_{86}P_4O_{22}Sn_2FeW_2 \cdot C_7H_8$ (2084.33 g/mol): C, 40.91; H, 4.55. Found: C, 40.5; H, 4.6%.

2.1.3. Synthesis of [4-t-Bu-2,6-{P(O)(O-i-Pr)$_2$}$_2$C$_6$H$_2$SnC$_5$H$_4$]$_2$Fe · Cr(CO)$_4$ (3)

Bicyclo[2.2.1]heptadiene chromium tetracarbonyl (0.107 g, 0.42 mmol) was added to a solution of [4-*t*-Bu-2,6-{P(O)(O-*i*-Pr)$_2$}$_2$C$_6$H$_2$SnC$_5$H$_4$]$_2$Fe (**1**) (0.564 g, 0.42 mmol) in *n*-hexane (70 ml). After the reaction mixture had been heated at reflux for 48 h the *n*-hexane was removed in vacuo. Toluene (30 ml) was added to the solid residue and the resulting mixture was stirred for 10 min followed by filtration. The filtrate was kept overnight at

Table 2
Selected bond lengths (Å), bond angles (°), and torsion angles (°) for **1** and **2**

	1	**2**
Sn(1)–C(11)	2.191(2)	2.139(6)
Sn(1)–C(1)	2.241(2)	2.195(5)
Sn(1)–O(1)	2.472(2)	2.366(4)
Sn(1)–O(2)	2.491(2)	2.426(3)
Sn(1)–W(1)	–	2.7692(5)
P(1)–O(1)	1.480(2)	1.488(4)
P(1)–O(1″)	1.568(2)	1.564(4)
P(1)–O(1′)	1.581(2)	1.573(4)
P(1)–C(2)	1.786(2)	1.772(5)
P(2)–O(2)	1.481(2)	1.479(3)
P(2)–O(2′)	1.565(2)	1.565(4)
P(2)–O(2″)	1.583(2)	1.567(4)
P(2)–C(6)	1.781(2)	1.787(5)
C(11)–Sn(1)–C(1)	91.80(7)	102.1(2)
C(11)–Sn(1)–O(1)	87.23(6)	91.5(2)
C(1)–Sn(1)–O(1)	76.14(6)	77.6(2)
C(11)–Sn(1)–O(2)	91.52(7)	87.8(2)
C(1)–Sn(1)–O(2)	75.97(6)	76.6(2)
O(1)–Sn(1)–O(2)	152.02(5)	153.5(1)
C(1)–C(2)–P(1)	115.4(2)	115.8(4)
C(1)–C(6)–P(2)	116.0(2)	115.3(4)
C(11)–Sn(1)–W(1)	–	126.4(1)
C(1)–Sn(1)–W(1)	–	131.4(1)
O(1)–Sn(1)–W(1)	–	102.32(9)
O(2)–Sn(1)–W(1)	–	99.4(8)
Sn(1)–C(1)–C(1A)–Sn(1A)	180.0	–
Sn(1)–C(1)–C(2)–C(3)	−179.3(2)	177.5(4)
O(1)–P(1)–C(2)–C(3)	−178.0(2)	−177.5(4)
O(2)–P(2)–C(6)–C(5)	−177.5(2)	178.0(5)

−30 °C to cause precipitation of compound **3** (0.361 g, 57%) as orange crystals which decompose at 160 °C.

^{1}H NMR (400.13 MHz, toluene-d^8): δ 0.97 (d, 12H, CH(CH_3)$_2$, J(^{1}H–^{1}H) = 6.3 Hz), 1.11 (s, 18H C(CH_3)$_3$), 1.16 (d, 12H, CH(CH_3)$_2$, J(^{1}H–^{1}H) = 6.3 Hz), 1.19 (d, 12H, CH(CH_3)$_2$, J(^{1}H–^{1}H) = 5.8 Hz), 1.46 (d, 12H, CH(CH_3)$_2$, J(^{1}H–^{1}H) = 5.8 Hz), 4.38 (s, 4H, C$_5H_4$), 4.53–4.57 (complex pattern, 4H, CH(CH$_3$)$_2$), 4.83 (s, 4H, C$_5H_4$), 5.33–5.38 (complex pattern, 4H, CH(CH$_3$)$_2$), 7.98 (d, 4H, CH_{aryl}, ^3J(^{31}P–^{1}H) = 13.3 Hz). ^{13}C{^{1}H} NMR (100.63 MHz, toluene-d^8): δ 23.3–23.4 (complex pattern, CH(CH$_3$)$_2$), 23.5 (complex pattern, CH(CH$_3$)$_2$), 24.0 (complex pattern, CH(CH$_3$)$_2$), 30.5 (s, C(CH$_3$)$_3$), 34.2 (s, C(CH$_3$)$_3$), 69.1 (s, C_5H_{4meta}), 71.2 (complex pattern, CH(CH$_3$)$_2$), 72.5 (complex pattern, CH(CH$_3$)$_2$), 74.6 (s, C_5H_{4ortho}), 90.6 (s, C_5H_{4ipso}), 131.0 (dd, $C_{3/5aryl}$, ^2J(^{13}C–^{31}P) = 15.6 Hz, ^4J(^{13}C–^{31}P) = 4.7 Hz), 133.4 (dd, $C_{2/6aryl}$, ^1J(^{13}C–^{31}P) = 187.6 Hz, ^3J(^{13}C–^{31}P) = 21.9 Hz), 150.4 (t, C_{4aryl}, ^3J(^{13}C–^{31}P) = 12.6 Hz), 176.1 (t, C_{1aryl}, ^2J-(^{13}C–^{31}P) = 29.2 Hz), 227.0 (s, CO), 237.0 (s, CO). ^{31}P{^{1}H} NMR (161.98 MHz, toluene-d^8): δ 29.3 (J(^{31}P–$^{119/117}$Sn) = 125.2 Hz). ^{119}Sn{^{1}H} NMR (149.21 MHz, toluene-d^8): δ 320.6 (J(^{31}P–^{119}Sn) = 129 Hz). IR (KBr): $\tilde{\nu}$ = 1194 cm^{-1} (P═O), 1827 cm^{-1} (CO), 1875 cm^{-1} (CO), 1974 cm^{-1} (CO). Mössbauer spectroscopy: I.S. = 1.98 mm/s, Q.S. = 3.92 mm/s. Elemental analyses calculated for $C_{58}H_{86}P_4O_{16}Sn_2CrFe$ (1508.45 g/mol): C, 46.18; H, 5.75. Found: C, 46.0; H, 5.9%.

*2.1.4. Reaction of [4-t-Bu-2,6-{P(O)(O-i-Pr)$_2$}$_2$C$_6$H$_2$SnC$_5$H$_4$]$_2$Fe (**1**) with sulphur*

At −78 °C, sulphur (19.6 mg, 0.62 mmol) was added to a magnetically stirred solution of [4-*t*-Bu-2,6-{P(O)(O-*i*-Pr)$_2$}$_2$C$_6$H$_2$SnC$_5$H$_4$]$_2$Fe (**1**) (0.418 g, 0.31 mmol) in THF (40 ml). The reaction mixture was stirred for a period of 6 h during which room temperature was reached. The solution was reduced in vacuo to a volume of 10 ml (hereafter referred to solution A) and then characterized by NMR spectroscopy.

^{31}P{^{1}H} NMR (121.49 MHz, THF, D$_2$O-capillary): δ 26.9–27.2 (not resolved, integral 11%), 24.6–25.4 (not resolved, integral 9%), 21.5 (s, $v_{1/2}$ = 18 Hz, integral 28%), 20.5 (s, $v_{1/2}$ = 19 Hz, integral 30%), 18.7 (s, J(^{31}P–$^{119/117}$Sn) = 30 Hz, integral 14%), 16.5 (s, integral 4%, **R**–**H**), 12.0–12.6 (not resolved, integral 5%). ^{119}Sn{^{1}H} NMR (111.92 MHz, THF, D$_2$O-capillary): δ −17, −25 (t, J(^{31}P–^{119}Sn) = 21 Hz), −129 (t, J(^{31}P–^{119}Sn) = 31 Hz).

Over a period of 4 d and contact with air moisture, solution A was slowly evaporated at room temperature. The residue was dissolved in acetonitrile (10 ml) to give solution B which was investigated by ^{31}P NMR spectroscopy.

^{31}P{^{1}H} NMR (161.98 MHz, CD$_3$CN): δ 23.3–25.6 (unresolved, integral 37%), 20.4 (s, $v_{1/2}$ = 19 Hz, integral 1.4%), 19.5 (s, $v_{1/2}$ = 32 Hz, integral 1.5%), 18.5 (s, $v_{1/2}$ = 19 Hz, integral 2.5%), 16.3 (s, $v_{1/2}$ = 35 Hz, integral 4%), 15.5 (s, integral 8%, **R**–**H**), 13.6 (s, integral 11%), 12.0–13.2 (unresolved, integral 37%).

Toluene (5 ml) was added to solution B. During slow evaporation under contact with air moisture from this solution the ferrocenyl-bridged sulphur-containing ladder-type compound **5** was formed as orange crystals (67 mg, 25%) which decompose above 200 °C.

^{1}H NMR (400.13 MHz, THF-d^8): δ 0.94 (d, 3H, CH(CH_3)$_2$, J(^{1}H–^{1}H) = 6.0 Hz), 1.24 (d, 3H, CH(CH_3)$_2$, J(^{1}H–^{1}H) = 6.3 Hz), 1.38 (d, 3H, CH(CH_3)$_2$, J(^{1}H–^{1}H) = 6.0 Hz), 1.45 (d, 3H, CH(CH_3)$_2$, J(^{1}H–^{1}H) = 6.3 Hz), 1.47 (s, 9H, C(CH_3)$_3$), 1.65 (d, 3H, CH(CH_3)$_2$, J(^{1}H–^{1}H) = 6.3 Hz), 1.68 (d, 3H, CH(CH_3)$_2$, J(^{31}P–^{1}H) = 6.0 Hz), 3.97 (s, 1H, C$_5H_4$), 3.99 (s, 1H, C$_5H_4$), 4.04 (s, 1H, C$_5H_4$), 4.11 (s, 1H, C$_5H_4$), 4.14 (s, 1H, C$_5H_4$), 4.30 (s, 1H, C$_5H_4$, J(^{1}H–$^{119/117}$Sn) = 21.1 Hz), 4.37–4.45 (complex pattern, 1H, OCH(CH$_3$)$_2$), 4.47 (s, 1H, C$_5H_4$), 4.85–4.92 (complex pattern, 1H, OCH(CH$_3$)$_2$), 5.10 (s, 1H, C$_5H_4$, J(^{1}H–$^{119/117}$Sn) = 16.1 Hz), 5.25–5.32 (complex pattern, 1H, OCH(CH$_3$)$_2$), 7.89 (d, 1H, CH_{aryl}, ^3J(^{31}P–^{1}H) = 13.5 Hz), 8.39 (d, 1H, CH_{aryl}, ^3J(^{31}P–^{1}H) = 14.1 Hz). ^{31}P{^{1}H} NMR (161.98 MHz, THF-d^8): δ 25.9 (d, J(^{31}P–^{31}P) = 8 Hz, J(^{31}P–$^{119/117}$Sn) = 17 Hz), 12.3 (d, J(^{31}P–^{31}P) = 8 Hz, J(^{31}P–$^{119/117}$Sn) = 94 Hz). Because of its poor solubility, attempts at obtaining a reasonable ^{119}Sn NMR spectrum failed. IR (KBr): $\tilde{\nu}$ = 1174 cm^{-1} (P═O), 1145 cm^{-1} (P═O).

Table 3
Selected bond lengths (Å), bond angles (°), and torsion angles (°) for **3**

Sn(1)–C(21)	2.160(4)	Sn(2)–C(26)	2.147(4)
Sn(1)–C(1)	2.209(4)	Sn(2)–C(11)	2.214(4)
Sn(1)–O(2)	2.410(2)	Sn(2)–O(3)	2.386(3)
Sn(1)–O(1)	2.412(2)	Sn(2)–O(4)	2.454(2)
Sn(1)–Cr(1)	2.6065(7)	Sn(2)–Cr(1)	2.5912(7)
P(1)–O(1)	1.487(3)	P(3)–O(3)	1.482(3)
P(1)–O(1′)	1.562(3)	P(3)–O(3″)	1.511(8)
P(1)–O(1″)	1.574(3)	P(3)–O(3′)	1.73(1)
P(1)–C(2)	1.778(4)	P(3)–C(12)	1.777(4)
P(2)–O(2)	1.486(3)	P(4)–O(4)	1.482(3)
P(2)–O(2′)	1.564(3)	P(4)–O(4″)	1.574(3)
P(2)–O(2″)	1.574(2)	P(4)–O(4′)	1.580(3)
P(2)–C(6)	1.787(4)	P(4)–C(16)	1.782(4)
C(21)–Sn(1)–C(1)	98.2(1)	C(26)–Sn(2)–C(11)	99.0(1)
C(21)–Sn(1)–O(2)	91.3(1)	C(26)–Sn(2)–O(3)	86.9(1)
C(1)–Sn(1)–O(2)	76.4(1)	C(11)–Sn(2)–O(3)	77.5(1)
C(21)–Sn(1)–O(1)	85.5(1)	C(26)–Sn(2)–O(4)	92.3(1)
O(1)–Sn(1)–O(2)	152.22(9)	O(4)–Sn(2)–O(3)	153.12(9)
C(21)–Sn(1)–Cr(1)	127.6(1)	C(26)–Sn(2)–Cr(1)	127.8(1)
C(1)–Sn(1)–Cr(1)	133.91(9)	C(11)–Sn(2)–Cr(1)	133.1(1)
O(1)–Sn(1)–Cr(1)	99.75(7)	O(4)–Sn(2)–Cr(1)	102.20(6)
O(2)–Sn(1)–Cr(1)	104.00(6)	O(3)–Sn(2)–Cr(1)	99.43(6)
C(1)–Sn(1)–O(1)	76.8(1)	C(11)–Sn(2)–O(4)	76.1(1)
Sn(1)–Cr(1)–Sn(2)	88.47(2)	C(57)–Cr(1)–Sn(1)	–
C(1)–C(2)–P(1)	114.6(3)	C(11)–C(12)–P(3)	115.0(3)
C(1)–C(6)–P(2)	115.1(3)	C(11)–C(16)–P(4)	115.3(3)
Sn(1)–C(1)–C(2)–C(3)	−178.3(3)	Sn(2)–C(11)–C(12)–C(13)	175,6(3)
O(1)–P(1)–C(2)–C(3)	166.8(3)	O(3)–P(3)–C(12)–C(13)	−171.0(3)
O(2)–P(2)–C(6)–C(5)	179.8(3)	O(4)–P(4)–C(16)–C(15)	175.9(3)

Elemental analyses calculated for $C_{58}H_{80}P_4O_{14}Sn_4Fe_2S_2$ (1775.80 g/mol): C, 39.23; H, 4.54. Found: C, 39.0; H, 4.7%.

Table 4
Selected bond lengths (Å) and bond angles (°) for **5**

Sn(1)–O(3)	2.035(5)	Sn(2)–O(3A)	2.056(6)
Sn(1)–C(11)	2.11(1)	Sn(2)–O(3)	2.072(6)
Sn(1)–C(1)	2.185(9)	Sn(2)–C(16)	2.07(1)
Sn(1)–O(1)	2.310(5)	Sn(2)–O(2)	2.181(6)
Sn(1)–S(1)	2.410(3)	Sn(2)–O(2′A)	2.188(6)
Sn(2)–Sn(2A)	3.260(1)	Sn(2)–S(1A)	2.519(2)
P(1)–O(1)	1.497(6)	P(2)–O(2)	1.502(6)
P(1)–O(1′)	1.553(6)	P(2)–O(2′)	1.511(7)
P(1)–O(1″)	1.563(6)	P(2)–O(2″)	1.575(7)
P(1)–C(2)	1.791(9)	P(2)–C(6)	1.816(9)
O(3)–Sn(1)–C(11)	91.1(3)	O(3A)–Sn(2)–O(3)	75.7(2)
O(3)–Sn(1)–C(1)	103.1(3)	O(3A)–Sn(2)–C(16)	172.4(3)
C(11)–Sn(1)–C(1)	121.1(4)	O(3)–Sn(2)–C(16)	96.7(3)
O(3)–Sn(1)–O(1)	174.9(2)	O(3A)–Sn(2)–O(2)	87.3(2)
C(11)–Sn(1)–O(1)	86.7(3)	O(3)–Sn(2)–O(2)	80.0(2)
C(1)–Sn(1)–O(1)	81.9(3)	C(16)–Sn(2)–O(2)	91.7(3)
O(3)–Sn(1)–S(1)	83.3(2)	O(3A)–Sn(2)–O(2′A)	82.3(2)
C(11)–Sn(1)–S(1)	129.7(3)	O(3)–Sn(2)–O(2′A)	82.8(2)
C(1)–Sn(1)–S(1)	108.8(2)	O(2)–Sn(2)–O(2′A)	161.6(2)
O(1)–Sn(1)–S(1)	94.6(2)	O(3A)–Sn(2)–S(1A)	80.1(2)
Sn(1)–S(1)–Sn(2A)	84.26(9)	O(3)–Sn(2)–S(1A)	155.7(2)
Sn(1)–O(3)–Sn(2A)	107.9(3)	C(16)–Sn(2)–S(1A)	107.5(3)
Sn(1)–O(3)–Sn(2)	144.4(3)	O(2)–Sn(2)–S(1A)	96.8(2)
Sn(2A)–O(3)–Sn(2)	104.3(2)	O(2′A)–Sn(2)–S(1A)	96.3(2)
C(6)–C(1)–Sn(1)	126.9(6)	C(1)–C(2)–P(1)	117.9(7)
C(2)–C(1)–Sn(1)	116.0(7)	C(1)–C(6)–P(2)	123.0(7)

3. Results and discussion

The reaction of the heteroleptic stannylene [4-*t*-Bu-2,6-{P(O)(O-*i*-Pr)$_2$}$_2$C$_6$H$_2$]SnCl with 1,1′-dilithioferrocene · TMEDA in the molar ratio 2:1 provided the ferrocenyl-bridged bis(diorganostannylene) [4-*t*-Bu-2,6-{P(O)(O-*i*-Pr)$_2$C$_6$H$_2$Sn}C$_5$H$_4$]$_2$Fe (**1**) in good yield (Eq. (1))

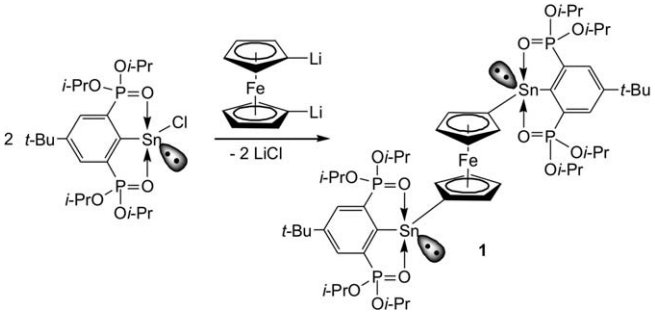

(1)

Compound **1** is an orange crystalline solid which is well soluble in organic solvents such as diethyl ether, dichloromethane, and toluene but much less soluble in aliphatic hydrocarbons. Compared to the heteroleptic stannylene [4-*t*-Bu-2,6-{P(O)(O-*i*-Pr)$_2$}$_2$C$_6$H$_2$]SnCl, compound **1** is much less stable towards oxidation and hydrolysis. The Mössbauer spectrum shows an isomer shift I.S. of 2.61 mm/s (Q.S. 4.01 mm/s) confirming the low-valence of the tin atom.

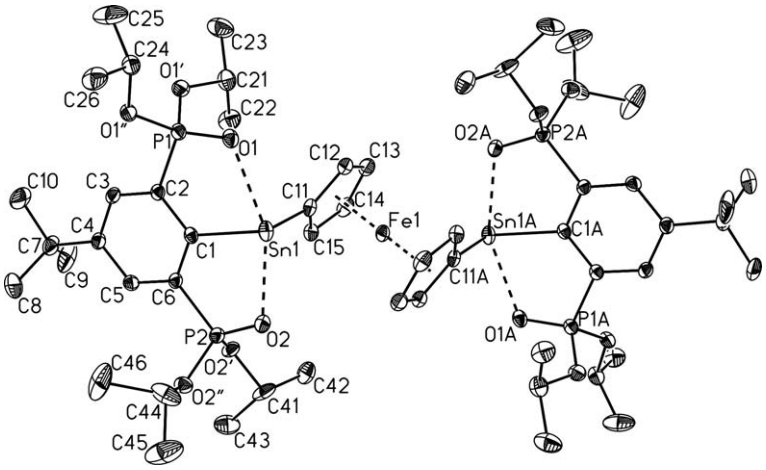

Fig. 1. General view (SHELXTL) of a molecule of **1** showing 30% probability displacement ellipsoids and the atom numbering (Symmetry transformations used to generate equivalent atoms: $A = 1 - X, 1 - Y, -Z$).

Single crystals suitable for X-ray diffraction analysis of compound **1** were obtained as toluene solvate **1** · 2 toluene from a toluene solution at −30 °C. The molecular structure of compound **1** is shown in Fig. 1 and selected geometric parameters are listed in Table 2.

The molecule shows a centre of inversion and consequently, both stannylene moieties are crystallographically equivalent and mutual *trans* with a Sn(1)–C(11)–C(11A)–Sn(1A) torsion angle of 180.0(1)°. The tin atom exhibits a strongly distorted ψ-trigonal bipyramidal configuration with C(1), C(11), and the lone pair occupying the equatorial and O(1) and O(2) occupying the axial positions, respectively. The C(1)–Sn(1)–C(11) angle of 91.80(7)° indicates high s-character of the lone pair and almost exclusive participation of p-orbitals for the Sn–C and Sn–O bonding. As result of the ligand constraint the O(1)–Sn(1)–O(2) angle deviates from the ideal value of 180° and amounts to 152.02(5)°. The intramolecular Sn(1)–O(1) and Sn(1)–O(2) distances of 2.472(2) and 2.491(2) Å, respectively, are longer than the corresponding distances in the parent compound {4-*t*-Bu-2,6-[P(O)(O-*i*-Pr)$_2$]$_2$C$_6$H$_2$}SnCl (2.423(2), 2.430(2) Å) [52]. Consequently, the P(1)–O(1) and P(2)–O(2) distances of 1.480(2) and 1.481(2) Å in compound **1** are only slightly longer than the corresponding ones in the protonated ligand 5-*t*-Bu-1,3-{P(O)(O-*i*-Pr)$_2$}$_2$C$_6$H$_3$ (1.470(3), 1.466 (3) Å) [52]. This situation is also reflected by the IR spectrum of compound **1** showing a $\tilde{\nu}$ (P=O) of 1199 cm^{-1}. The distances between the iron atom and the ferrocene carbon atoms vary between 2.035(2) and 2.070(2) Å and correspond to the values measured for the organotin(IV)-substituted derivatives {μ2-(Cp$_2$Fe-1,1′-diyl)–Sn(*t*-Bu)$_2$}$_2$ (2.077–2.076 Å) and {μ2-(Cp$_2$Fe-1,1′-diyl)–Sn(Mes)$_2$}$_2$ (2.066–2.077 Å) [49,50].

The identity of compound **1** was also confirmed by its ^{1}H, ^{13}C, ^{31}P, and ^{119}Sn NMR spectra (see Section 2). Most remarkably, the ^{1}H NMR spectrum shows four equally intense resonances for the methyl protons of the *i*-propyl groups which is indicative for the stereochemical activity of the lone pair at the tin atom.

Under UV-light irradiation, the reaction of compound **1** with tungsten hexacarbonyl, W(CO)$_6$, provided the corresponding transition metal complex [4-*t*-Bu-2,6-{P(O)(O-*i*-Pr)$_2$}$_2$C$_6$H$_2$Sn{W(CO)$_5$}C$_5$H$_4$]$_2$Fe (**2**) as orange crystalline solid in good yield (Eq. (2))

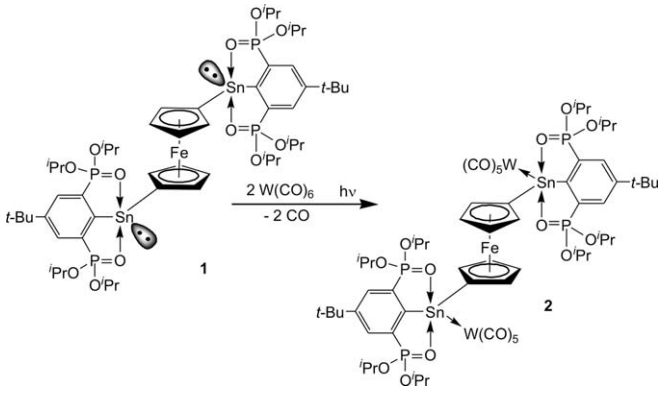

(2)

Single crystals suitable for X-ray diffraction analysis of compound **2** were obtained as toluene solvate **2** · 2 toluene by slow evaporation at room temperature of a toluene solution. The molecular structure is shown in Fig. 2 and selected bond distances and bond angles are listed in Table 2.

Like compound **1**, its tungsten pentacarbonyl complex **2** is centrosymmetric with the stannylene moieties mutual *trans*. The Sn(1) atom shows a distorted trigonal bipyramidal configuration (geometrical goodness [57,58] $\Delta\Sigma(\theta) = 88.5°$) with C(1), C(11), and W(1) in the equatorial and O(1) and O(2) in the axial positions. The Sn(1) atom is displaced, in direction of O(1), by 0.053(2) Å from the plane defined by C(1), C(11), W(1). Most remarkably, in compound **2** the tin–carbon as well as the tin–oxygen distances are significantly shorter than the corresponding distances in compound **1** (see Table 1). Apparently, the tungsten

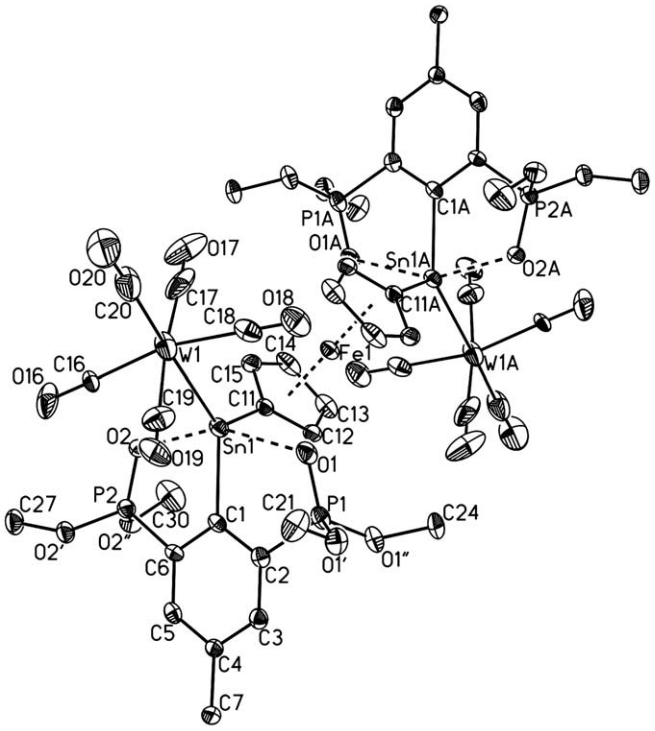

Fig. 2. General view (SHELXTL) of a molecule of **2** showing 30% probability displacement ellipsoids and the atom numbering (Symmetry transformations used to generate equivalent atoms: $A = 0.5 - X, 0.5 - Y, -Z$). All methyl groups are omitted for clarity.

pentacarbonyl moiety reduces the electron density at the tin atom. The Sn(1)–W(1) distance amounts to 2.7692(5) Å which is comparable to the corresponding distances in $(o\text{-}C_6H_4CH_2NMe_2)_2SnW(CO)_5$ (Sn–W 2.749(1) Å) and $(o\text{-}C_6H_4CH_2PPh_2)_2SnW(CO)_5$ (Sn–W 2.762(1) Å) [59].

The ^1H, ^{13}C, ^{31}P, and ^{119}Sn NMR data (see Section 2) confirm the identity of compound **2** in solution. Like for compound **1**, the diastereotopism of the *i*-propyl groups is reflected by two equally intense multiplets for the CH-protons and four equally intense doublets for the methyl protons.

The reaction of compound **1** with bicyclo[2.2.1]heptadiene-chromium tetracarbonyl, $C_7H_8Cr(CO)_4$, at 60 °C provided the corresponding transition metal complex [4-*t*-Bu-2,6-$\{P(O)(O\text{-}i\text{-}Pr)_2\}_2C_6H_2SnC_5H_4]_2Fe \cdot Cr(CO)_4$ (**3**) as orange crystalline solid in good yield (Eq. (3))

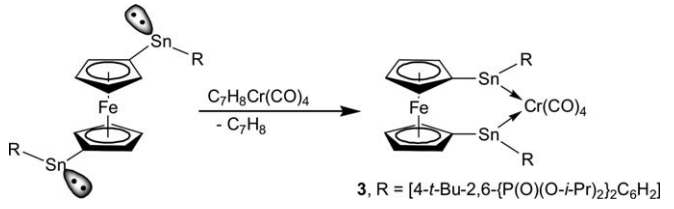

(3)

The Mössbauer spectrum of compound **3** shows an isomer shift I.S. of 1.98 mm/s (Q.S. 3.92 mm/s) being smaller than that observed for the parent compound **1** (see above). This is to be expected as the s-electron density at the tin atoms in compound **3** is used for the Sn–Cr bonds. Single crystals suitable for X-ray diffraction analysis of compound **3** were obtained as toluene solvate **3** · 2.5 toluene from a toluene solution at 0 °C. The molecular structure is shown in Fig. 3 and selected bond distances and bond angles are listed in Table 3.

In compound **3**, the tin atoms Sn(1) and Sn(2) coordinate to the chromium atom and form a chelate ring involving these atoms and the ferrocene moiety. The torsion angle Sn(1)–centroid(1)–centroid(2)–Sn(2) amounts to 35.4(1)°. Apparently, the barrier to rotation of the cyclopentadienyl rings (hereafter referred to as Cp) at the Cp–Fe–Cp axis is low and allows such a reorientation from the *trans*-conformation observed in compound **1** to the *cis*-conformation in compound **3**. The Sn(1)–Cr(1) and Sn(2)–Cr(1) distances amount to 2.6065(7) and 2.5912(7) Å, respectively, and resemble those found in $\{(Me_3Si)_2CH\}_2SnCr(CO)_5$ (2.562(5) Å) [60] and ArAr′$SnCr(CO)_5$ (Ar = 1,3,5-*t*-BuC_6H_2; Ar′ = $CH_2C(CH_3)_2$-3,5-*t*-$Bu_2C_6H_2$) (2.61(4) Å) [61]. The torsion angle Sn(1)–Cr(1)–Sn(2)–Fe(1) amounts to 0.05(2)° and indicates that these metal atoms lie almost perfectly in a plane (see Fig. 4).

Notably, the intramolecular Sn(1)···Sn(2) distance amounts to 3.626(3) Å which is shorter than the sum of the van der Waals radii of two tin atoms (4.40 Å) [62] and which is comparable to the tin–tin distance of 3.639 Å reported for $[\{2,4,6\text{-}(CF_3)_3C_6H_2\}_2Sn]_2$ [63].

Both tin atoms Sn(1) and Sn(2) are crystallographically independent but show, however, rather similar distorted trigonal bipyramidal configurations (geometrical goodness [57,58] $\Delta\Sigma(\theta) = 88.0°$(Sn1), 89.3°(Sn2)). The equatorial positions are occupied by C(1), C(21) and Cr(1) (at Sn1), and C(11), C(26) and Cr(1) (at Sn2), respectively. The axial positions are occupied by O(1), O(2) (at Sn1), and O(3), O(4) (at Sn2). The intramolecular Sn(1)–O(1) (2.412(2) Å) and Sn(1)–O(2) (2.410(2) Å) distances are almost equal whereas the Sn(2)–O(3) (2.386(3) Å) and Sn(2)–O(4) (2.454(2) Å) distances differ by 0.068 Å. The O(1)–Sn(1)–O(2) and O(3)–Sn(2)–O(4) angles of 152.22(9)° and 153.12(9)°, respectively, are rather close to the corresponding angles in compounds **1** and **2**. Like in compound **2** but to less extent, the C(1)–Sn(1)–C(21) and C(11)–Sn(2)–C(26) angles of 98.2(1)° and 99.0(1)°, respectively, are enlarged as compared to the related angles in compound **1**.

The ^1H, ^{13}C, ^{31}P, and ^{119}Sn NMR data (see Section 2) confirm the identity of compound **3** in solution, including the diastereotopism of the *i*-propyl groups.

A typical reaction stannylenes easily undergo is the oxidative addition with sulphur. The reaction of the heteroleptic stannylene [4-*t*-Bu-2,6-$\{P(O)(OEt)_2\}_2C_6H_2$]SnCl with sulphur provided [4-*t*-Bu-2,6-$\{P(O)(OEt)_2\}_2C_6H_2$](Cl)SnS which is a dimer in the solid state containing a Sn_2S_2-four-membered ring [41]. For the reaction of compound **1** with two molar equivalents of sulphur in thf we expected formation of a sulphur-containing ferrocenophane-type compound **4** which, however, could not be identified (Scheme 1).

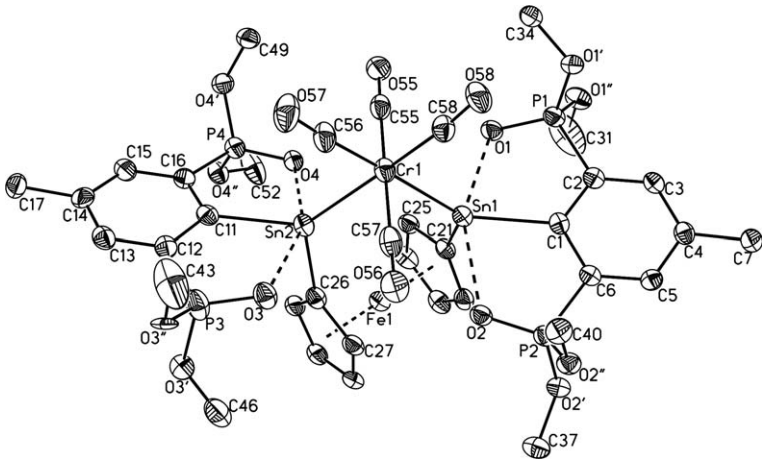

Fig. 3. General view (SHELXTL) of a molecule of **3** showing 30% probability displacement ellipsoids and the atom numbering scheme. All methyl groups are omitted for clarity.

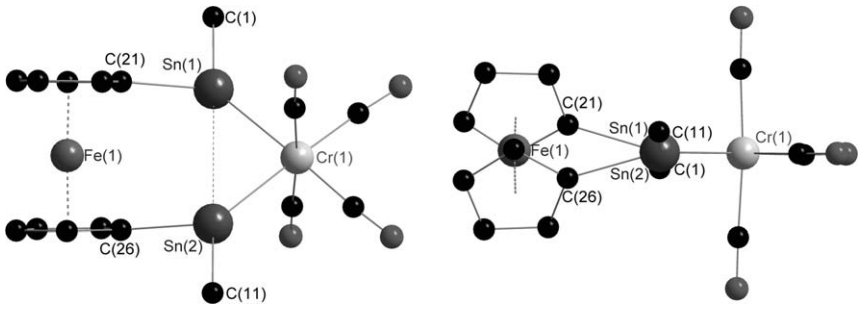

Fig. 4. View of compound **3** along the cyclopentadienyl plane (left) and along the Sn(1)–Sn(2) axis (right). The pincer-type ligands are omitted for clarity.

Instead, from the reaction mixture from which, under contact with air moisture, the solvent had slowly been evaporated and the residue had been re-dissolved in acetonitrile, orange crystals of the tetranuclear organotin compound **5** were obtained (Scheme 1). Compound **5** is almost insoluble in dichloromethane, chloroform, and benzene but poorly soluble in tetrahydrofurane and acetonitrile. No detailed studies concerning the mechanism for the formation of compound **5** was performed. One possible *formal* reaction sequence which appears to be feasible is shown in Scheme 2.

The product of the oxidative addition of sulphur to stannylene **1** immediately undergoes hydrolysis to give a ferrocenyl-bridged bis(diorganohydroxomercaptostannane). This dimerises under cleavage of two tin–carbon bonds (formation of 2 R–H), and elimination of two water and two *i*-propyl mercaptane molecules. This idea gets support by unambiguous detection of R–H in the ^{31}P NMR spectrum of the crude reaction mixture (see Section 2) and the typical smell of mercaptane in course of the reaction. Single crystals suitable for X-ray diffraction analysis of compound **5** were obtained as toluene solvate **5** · 3 toluene by slow evaporation of a toluene/THF-solution. The molecular structure is shown in Fig. 5 and selected bond distances and bond angles are listed in Table 4.

Compound **5** is centrosymmetric and shows a $Sn_4O_2S_2$ ladder-type structural motif in which two Sn_2OS four-membered rings are connected to a central Sn_2O_2 four-membered ring. This arrangement resembles that of [(*cyclo*-hexyl)$_2$ClSnOSn(SH)(*cyclo*-hexyl)$_2$]$_2$ [64]. The $Sn_4O_2S_2$ structural motif is planar to ±0.1686 Å. The Sn–O distances within the ladder motif are rather similar and vary between 2.035(5) Å (Sn1–O3) and 2.072(6) Å (Sn2–O3). The Sn(1)–S(1) distance of 2.410(3) Å is by 0.109 Å shorter than the Sn(2)–S(1A) distance. Notably, the intramolecular Sn(2)···Sn(2A) distance of 3.260(1) Å is much shorter than twice the van der Waals radius [62] of a tin atom (4.40 Å).

The Sn(1) atom is five-coordinate and shows a distorted trigonal bipyramidal configuration (geometrical goodness [57,58] $\Delta\Sigma(\theta) = 82.1°$) with C(1), C(11), and S(1) occupying the equatorial, and O(1) and O(3) occupying the axial positions. The Sn(1) atom is displaced by 0.082(2) Å in direction of O(3) from the equatorial plane defined by C(1), C(11), S(1). The intramolecular Sn(1)–O(1) distance amounts to 2.310(5) Å and indicates strong coordination of the phosphonyl oxygen.

The Sn(2) atom is six-coordinate by one carbon atom, four oxygen atoms, and one sulphur atom, and exhibits a distorted octahedral configuration. The *trans* angles vary between 172.4(3)° (C16–Sn2–O3A) and 155.7(2)° (O3–

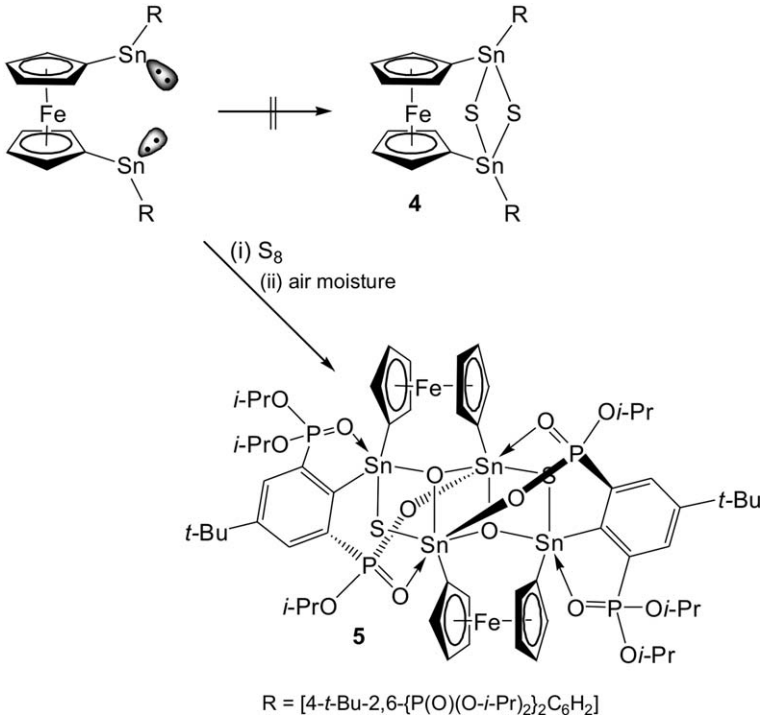

Scheme 1.

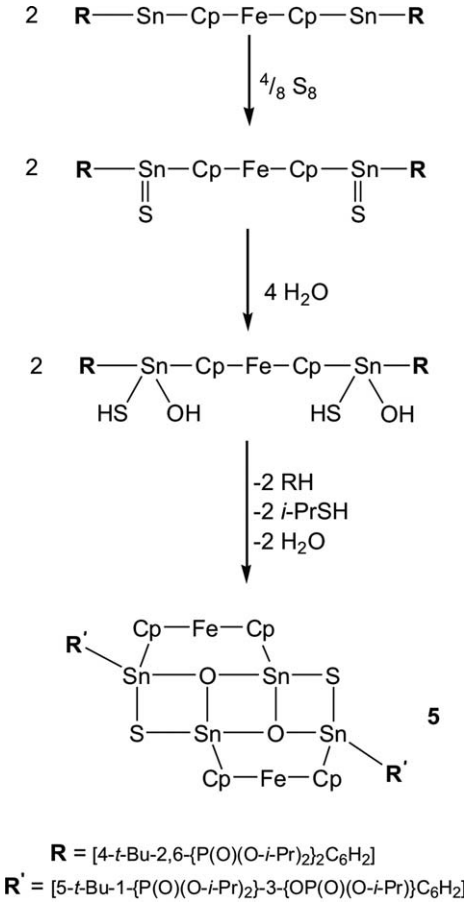

Scheme 2.

Sn2–S1A). The intramolecular Sn(2)–O(2) and Sn(2)–O(2′)A distances of 2.181(6) and 2.188(6) Å, respectively, are almost equal and rather short indicating isobidentate coordination mode of the RP(O*i*-Pr)(O)O$^-$ phosphonate moiety.

The Sn(1) and Sn(2) atoms are involved in different ring structures which are shown in a simplified manner in Chart 2.

3.1. Electrochemistry

The redox activity of complexes **1**–**3** has been investigated by electrochemical techniques in THF solution.

As expected, complex **1** exhibits the typical ferrocene-centred oxidation with features of chemical reversibility ($E^{0'} = +0.31$ V). Minor anodic processes are also present at more positive potential values, but they are confidently assigned to traces of by-products present in the original product. In fact, not only {4-*t*-Bu-2,6-[P(O)(O-*i*-Pr)$_2$]$_2$-C$_6$H$_2$}SnCl does not exhibit any oxidation process, but the current function ($i_{pa} \cdot v^{-1/2}$) for such steps maintains constant with scan rate, thus ruling out that they might originate from the **1**/[**1**]$^+$ process. On the other hand, exhaustive one-electron oxidation makes the original yellow solution to turn blue ($\lambda_{max} = 630$ nm) and the resulting solution displays a cyclic voltammetric response complementary to the original one, thus testifying to the chemical stability of [**1**]$^+$. Finally, as a consequence of the linkage of the stannylene fragment to ferrocene, no reduction process was detected

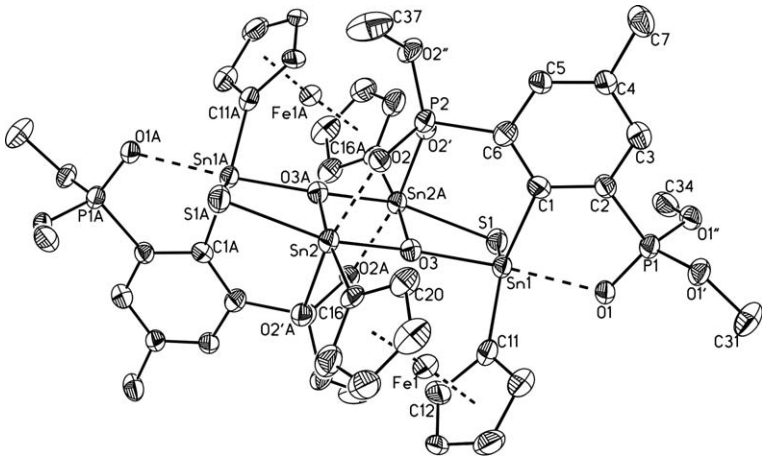

Fig. 5. General view (SHELXTL) of a molecule of **5** showing 30% probability displacement ellipsoids and the atom numbering (Symmetry transformations used to generate equivalent atoms: $A = -X, -Y, -Z$). All methyl groups are omitted for clarity.

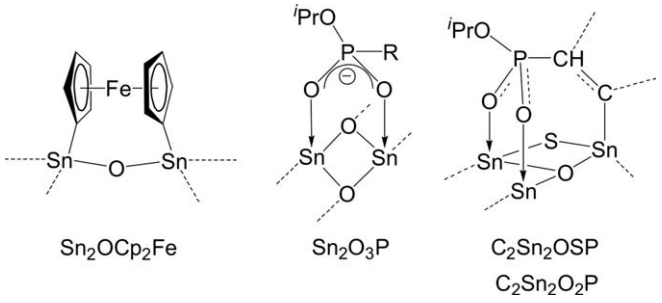

Chart 2.

for compound **1**, whereas {4-*t*-Bu-2,6-[P(O)(O-*i*-Pr)$_2$]$_2$-C_6H_2}SnCl affords an irreversible reduction ($E_p = -1.8$ V).

A qualitatively similar behaviour is displayed by complex **2**, even if exhaustive electrolysis in correspondence of the ferrocene/ferrocenium process ($E^{0'} = +0.43$ V) consumes 1.3 electrons *per* molecule. We are keen to attribute the extra-electron consumption to the tendency of the blue ferrocenium complex $[\mathbf{2}]^+$ ($\lambda_{max} = 625$ nm) to re-reduce, rather than to the partial involvement of W-centred processes. In fact, for instance, (*p*-MeOC_6H_4-DAB)W(CO)$_4$ (DAB = diazabutadiene) exhibits an irreversible metal-centred multi-electron oxidation at +0.73 V [65].

Finally, as illustrated in Fig. 6, complex **3** affords a more complex redox pattern. It undergoes two anodic processes ($E^{0'} = +0.18$ V and +0.48 V, respectively) both featuring partial chemical reversibility in the cyclic voltammetric time scale.

Controlled potential coulometry proves that the first process consumes one-electron *per* molecule. Concerning the second process, at different scan rates it displays peak-heights constantly about twice those of the first process. On this basis, it is conceivably assigned as a two-electron process. In this picture, we attribute the first process as ferrocene-centred, whereas, analogously to (*p*-MeOC_6H_4-DAB)Cr(CO)$_4$ [65], which displays a partially chemically reversible two-electron oxidation ($E_p = +0.43$ V), the second process is assigned as Cr-centred.

Analysis [66] of the cyclic voltammetric responses with scan rates varying from 0.02 V s^{-1} to 2.00 V s^{-1} also confirms that both the processes are accompanied by chemical complications. In fact, in both cases the respective current ratios i_{pc}/i_{pa} are constantly lower than 1 (for instance, at 0.05 V s^{-1}, the ratio is 0.5 for the first process and 0.6 for the second process).

Further confirming the instability of the oxidized products, the solution resulting from exhaustive one-electron oxidation ($E_w = +0.3$ V) assumes a yellow colour slightly darker than that of **3** and no more displays traces of the original cyclic voltammetric pattern.

As a final consideration, we underline that the stannylene moieties in compounds **1**–**3** push, even if at different extents, electron density towards the ferrocene core making the oxidation easier than that of unsubstituted ferrocene ($E^{0'} = +0.51$ V). This electron-donating ability of stannylene moieties, however, obviously depends in turn upon the inductive effects of the substituents attached to the tin atom. Thus, for instance, the oxidation potential of (C_5H_5)-

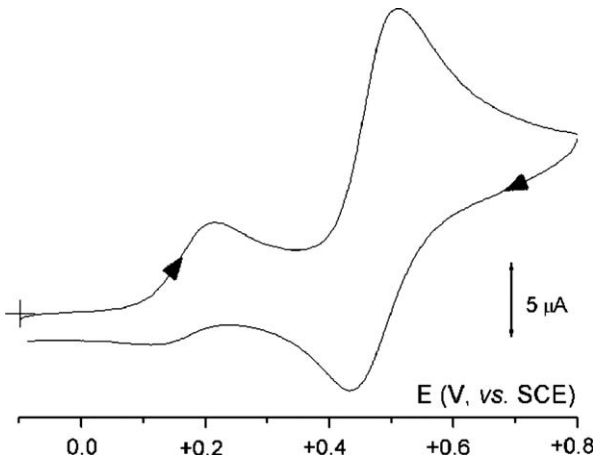

Fig. 6. Cyclic voltammogram recorded at a platinum electrode in THF-solution of **3** (1.0×10^{-3} mol dm^{-3}). [NBu_4][PF_6] (0.2 mol dm^{-3}) supporting electrolyte. Scan rate: 0.2 V s^{-1}.

$Fe(C_5H_3\text{-}CH_2N(Me)_2)SnCl_3$ containing the electron-withdrawing trichlorostannyl moiety is higher than that of unsubstituted ferrocene as well as of $(C_5H_5)Fe(C_5H_4\text{-}CH_2N(Me)_2)$ [35].

4. Conclusion

In this report, we have demonstrated the capacity of the heteroleptic stannylene [4-*t*-Bu-2,6-{P(O)(O-*i*-Pr)$_2$}$_2$C$_6$H$_2$]-SnCl for the high-yield synthesis of the first ferrocenyl-bridged bis(diorganostannylene) [4-*t*-Bu-2,6-{P(O)-(O-*i*-Pr)$_2$}$_2$C$_6$H$_2$SnC$_5$H$_4$]$_2$Fe (**1**). In a *proof of principle*-approach it was shown that compound **1** can act both as a bis-monodentate and bidentate-chelating ligand towards transition metal fragments such as $W(CO)_5$ and $Cr(CO)_4$, respectively. The fact that the germanium- and lead-analogues [67,68] of [4-*t*-Bu-2,6-{P(O)(O-*i*-Pr)$_2$}$_2$C$_6$-H$_2$]-SnCl are also in our hands makes the synthesis as well as complexation studies of [4-*t*-Bu-2,6-{P(O)(O-*i*-Pr)$_2$}$_2$C$_6$H$_2$MC$_5$H$_4$]$_2$Fe (M = Ge, Pb) a worthwhile goal, and this even more so when considering the enormous and ongoing interest in carbene-type ligands involving chelating bi- and tridentate ones and their application in transition metal chemistry [69]. Furthermore, based on the concept shown for the synthesis of compound **1**, the design of related bi- and even tridentate heavy carbene analogues-containing ligands appears to be feasible.

5. Supplementary material

Crystallographic data for the analysis have been deposited with the Cambridge Crystallographic Data Centre, CCDC Nos. 292003 (**1**), 292004 (**2**), 292005 (**3**), 292006 (**5**). Copies of this information may be obtained free of charge from The Director, CCDC, 12 Union Road, Cambridge, CB2 1EZ, UK (fax: +44 1223 336 033; e-mail: deposit@ccdc.cam.ac.uk or http://www.ccdc.cam.ac.uk).

Acknowledgements

We are grateful to the Deutsche Forschungsgemeinschaft and the Fonds der Chemischen Industrie for financial support. P.Z. acknowledges the financial support of the University of Siena (PAR 2005).

References

[1] E.O. Fischer, H. Grubert, Z. Naturforsch. (B) 11 (1956) 423.
[2] E.O. Fischer, H. Grubert, Z. Anorg. Allg. Chem. 286 (1956) 237.
[3] D.E. Goldberg, P.B. Hitchcock, M.F. Lappert, K.M. Thomas, J. Chem. Soc., Chem. Commun. (1976) 261.
[4] T. Fjeldberg, A. Haaland, B.E.R. Schilling, M.F. Lappert, A. Thorne, J. Chem. Soc., Dalton Trans. (1986) 1551.
[5] R. West, D.F. Moser, M. Haaf, T.A. Schmedake, I. Guzei, New reactions of stable silylenes, in: N. Auner, N. Weis (Eds.), Organosilicon Chemistry V: From Molecules to Materials, Wiley-VCH, New York, 2003, pp. 19–26.
[6] N.J. Hill, R. West, J. Organomet. Chem. 689 (2004) 4165.
[7] M. Kira, J. Organomet. Chem. 689 (2004) 4475.
[8] N. Tokitoh, W. Ando, React. Intermed. Chem. (2004) 651.
[9] M. Okasaki, H. Tobita, H. Ogino, Dalton Trans. (2003) 493.
[10] P.P. Gaspar, D. Zhou, Sci. Synth. 4 (2002) 135.
[11] B. Gehrhus, M.F. Lappert, J. Organomet. Chem. 617–618 (2001) 209.
[12] M. Haaf, T.A. Schmedake, R. West, Accounts Chem. Res. 33 (2000) 704.
[13] O. Kuhl, Coord. Chem. Rev. 248 (2004) 411.
[14] N. Takeda, N. Tokitoh, R. Okazaki, Sci. Synth. 5 (2003) 51.
[15] N. Tokitoh, R. Okazaki, Coord. Chem. Rev. 210 (2000) 251.
[16] J. Satge, Chem. Heterocyclic Comp. 35 (2000) 1013.
[17] N. Takeda, N. Tokitoh, R. Okazaki, Sci. Synth. 5 (2003) 311.
[18] K. Klinkhammer, Recent advances in structural chemistry of organic germanium, tin, and lead compounds, in: Z. Rappoport (Ed.), Chemistry of Organic Germanium, Tin, and Lead Compounds, vol. 2, Wiley, New York, 2002, p. 283 (Part 1).
[19] P. Jutzi, A. Mix, B. Rummel, W.W. Schoeller, B. Neumann, H.G. Stammler, Science 305 (2004) 849.
[20] M. Weidenbruch, J. Schlaefke, A. Schafer, K. Peters, H.G. von Schnering, H. Marsmann, Angew. Chem., Int. Ed. Engl. 33 (1994) 1846.
[21] R.S. Simons, L.H. Pu, M.M. Olmstead, P.P. Power, Organometallics 16 (1997) 1920.
[22] M. Saito, N. Tokitoh, R. Okazaki, Organometallics 15 (1996) 4531.
[23] C. Eaborn, M.S. Hill, P.B. Hitchcock, D. Patel, J.D. Smith, S.B. Zhang, Organometallics 19 (2000) 49.
[24] M. Kira, R. Yauchibara, R. Hirano, C. Kabuto, H. Sakurai, J. Am. Chem. Soc. 113 (1991) 7785.
[25] K. Angermund, K. Jonas, C. Krüger, J.L. Latten, Y.-H. Tsay, J. Organomet. Chem. 353 (1988) 17.
[26] J.T.B.H. Jastrzebski, P.A. van der Schaaf, J. Boersma, G. van Koten, D. Heijdenrijk, K. Goubitz, D.J.A. de Ridder, J. Organomet. Chem. 367 (1989) 55.
[27] J.T.B.H. Jastrzebski, G. van Koten, Adv. Organomet. Chem. 35 (1993) 241.
[28] J.T.H.B. Jastrzebski, D.M. Grove, J. Boersma, G. van Koten, J.-M. Ernsting, Mag. Reson. Chem. 29 (1991) 25.
[29] L.M. Engelhardt, B.S. Jolly, M.F. Lappert, C.L. Raston, A.H. White, J. Chem. Soc., Chem. Commun. (1988) 336.
[30] C. Drost, P.B. Hitchcock, M.F. Lappert, L.J.M. Pierssens, Chem. Commun. (1997) 1141.
[31] C. Drost, B. Gehrhus, P.B. Hitchcock, M.F. Lappert, Chem. Commun. (1997) 1845.
[32] C. Drost, P.B. Hitchcock, M.F. Lappert, Organometallics 17 (1998) 3838.
[33] C. Drost, P.B. Hitchcock, M.F. Lappert, Organometallics 21 (2002) 2095.
[34] B.S. Jolly, M.F. Lappert, L.M. Engelhardt, A.H. White, C.L. Raston, J. Chem. Soc., Dalton Trans. (1993) 2653.
[35] K. Jacob, N. Seidel, F. Voigt, A. Fischer, C. Pietzsch, J. Holecek, A. Lycka, M. Fontani, E. Grigiotti, P. Zanello, J. Prakt. Chem. 342 (2000) 574.
[36] S. Wingerter, H. Gornitzka, R. Bertermann, S.K. Pandey, J. Rocha, D. Stalke, Organometallics 19 (2000) 3890.
[37] J.T.B.H. Jastrzebski, P.A. van der Schaaf, J. Boersma, G. van Koten, Organometallics 8 (1989) 1373.
[38] K. Jurkschat, C. Klaus, M. Dargatz, A. Tzschach, J. Meunier-Piret, B. Mahieu, Z. Anorg. Allg. Chem. 577 (1989) 122.
[39] W.P. Leung, W.-H. Kwok, F. Xue, T.C.W. Mak, J. Am. Chem. Soc. 119 (1997) 1145.
[40] W.P. Leung, W.H. Kwok, L.-H. Erng, L.T.C. Law, Z.Y. Zhou, T.C.W. Mak, J. Chem. Soc., Dalton Trans. (1997) 4301.
[41] M. Mehring, C. Löw, M. Schürmann, F. Uhlig, K. Jurkschat, B. Mahieu, Organometallics 19 (2000) 4613.
[42] B.E. Eichler, P.P. Power, J. Am. Chem. Soc. 122 (2000) 8785.

[43] C.J. Cardin, D.J. Cardin, S.P. Constantine, A.K. Todd, S.J. Teat, S. Coles, Organometallics 17 (1998) 2144.
[44] H. Braunschweig, C. Drost, P.B. Hitchcock, M.F. Lappert, L.J.M. Pierssens, Angew. Chem., Int. Ed. Engl. 36 (1997) 261.
[45] W.P. Leung, Z.X. Wang, H.W. Li, Q.C. Yang, T.C.W. Mak, J. Am. Chem. Soc. 123 (2001) 8123.
[46] W.-P. Leung, Z.-X. Wang, H.-W. Li, T.C.W. Mak, Angew. Chem. 113 (2001) 2569.
[47] K. Jurkschat, M. Mehring, in: Z. Rappoport (Ed.), The chemistry of organic germanium, tin and lead compounds, vol. 2, Wiley, Chichester, 2002, p. 1543, and references cited.
[48] R.D. Archer, Inorganic and Organometallic Polymers, vol. 1, Wiley, New York, 2001, and references cited.
[49] R. Rulkens, A.J. Lough, I. Manners, Angew. Chem. 108 (1996) 1929.
[50] F. Jäkle, R. Rulkens, G. Zech, D.A. Foucher, A.J. Lough, I. Manners, Chem. Eur. J. 4 (1998) 2117.
[51] A.F. Fabrizi de Biani, M. Corsini, P. Zanello, H. Yao, M.E. Bluhm, R.N. Grimes, J. Am. Chem. Soc. 126 (2004) 11360.
[52] M. Henn, Ph.D. Thesis, Dortmund University, 2004..
[53] G.M. Sheldrick, Acta Crystallogr. Sect. A 46 (1990) 467.
[54] G.M. Sheldrick, University of Göttingen, 1997..
[55] International Tables for X-ray Crystallography, vol. C, Kluwer Academic Publishers, Dordrecht, 1992..
[56] G.M. Sheldrick, SHELXTL (Release 5.1, Software Reference Manual), Bruker AXS Inc., Madison, WI, USA, 1997.
[57] U. Kolb, M. Beuter, M. Dräger, Inorg. Chem. 33 (1994) 4522.
[58] M. Beuter, U. Kolb, A. Zickgraf, E. Bräu, M. Bletz, M. Dräger, Polyhedron 16 (1997) 4005.
[59] H.-P. Abicht, K. Jurkschat, A. Tzschach, K. Peters, E.-M. Peters, H.G. von Schnering, J. Organomet. Chem. 326 (1987) 357.
[60] J.D. Cotton, P.J. Davidson, D.E. Goldberg, M.F. Lappert, K.M. Thomas, J. Chem. Soc., Chem. Commun. (1974) 267.
[61] M. Weidenbruch, A. Stilter, K. Peters, H.G. von Schnering, Z. Anorg. Allg. Chem. 622 (1996) 534.
[62] J. Huheey, E.A. Keiter, R.L. Keiter, Anorganische Chemie: Prinzipien von Struktur und Reaktivität, second ed., Walter de Gruyter, Berlin, New York, 1995.
[63] U. Lay, H. Pritzkow, H. Grützmacher, J. Chem. Soc., Chem. Commun. (1992) 260.
[64] O.R. Flock, M. Dräger, Organometallics 12 (1993) 4623.
[65] B. Bildstein, M. Malaun, H. Kopacka, M. Fontani, P. Zanello, Inorg. Chim. Acta 300–302 (2000) 16.
[66] P. Zanello, Inorganic electrochemistry, Theory, Practice and Application, RSC, United Kingdom, 2003..
[67] K. Jurkschat, in: 11th International Conference on the Coordination and Organometallic Chemistry of Germanium, Tin, and Lead, ICCOC-GTL-11, Santa Fe, New Mexico, USA, Book of Abstracts O54, 27 June–2 July, 2004..
[68] K. Jurkschat, K. Peveling, M. Schürmann, Eur. J. Inorg. Chem. (2003) 3563.
[69] G. Bertrand, J. Organomet. Chem. 690 (2005) 5397, and articles published in this issue.